

Discrete states of conduction electrons bound to magnetoacceptors in quantum wells

S. Bonifacie, Y. M. Meziani, S. Juillaguet, C. Chaubet, and A. Raymond

Groupe d'Etude des Semiconducteurs, UMR CNRS 5650, Université Montpellier II, 34095 Montpellier, France

W. Zawadzki

Institute of Physics, Polish Academy of Sciences, 02668 Warsaw, Poland

V. Thierry-Mieg

Laboratoire de Photonique et de Nanostructures, CNRS, 91460 Marcoussis, France

J. Zeman

Laboratoire des Champs Magnétiques Intenses, CNRS, 38042 Grenoble, France

(Received 31 July 2003; published 20 October 2003)

Discrete states of conduction electrons bound to ionized acceptors are observed in intraband magneto-optical experiments on Be-doped GaAs/Ga_{0.67}Al_{0.33}As quantum wells. The electrons are bound to acceptors by a joint effect of the quantum well and an external magnetic field. The observed transition energies are successfully described using states of single magnetoacceptors. The energies show evidence for oscillatory screening of acceptor potentials. Also, two disorder modes of the cyclotron resonance related to acceptor potential fluctuations are observed at higher filling factors.

DOI: 10.1103/PhysRevB.68.165330

PACS number(s): 79.60.Jv, 76.40.+b, 61.72.Vv

I. INTRODUCTION

Cyclotron resonance (CR) experiments have been a powerful tool for years in the studies of two-dimensional electron gas (2DEG) in semiconductor heterostructures. Magneto-optical data are sensitive to particularities of the band structure, presence of impurities, and multielectron effects. The presence of donors in a quantum well (QW) results in additional magneto-optical transitions, which can be attributed to single impurities. On the other hand, samples containing intentional or residual acceptors exhibited until present only a disorder-shifted CR-like excitation observed by many authors, first on Si-MOS structures^{1–3} and then on the GaAs/Ga_{1–x}Al_xAs heterostructures.^{4–9} A simple interpretation of this CR like excitation is that the ionized acceptors provide potential fluctuations forming approximately parabolic wells. Such a well acts as a harmonic oscillator with a characteristic frequency ω_i . However, in a sample doped in the well with acceptors, one should also observe transitions related to single impurities, similar to the case of donors. Kubisa and Zawadzki¹⁰ proposed and described the discrete states of conduction electrons bound to ionized acceptors in heterostructures in the presence of a magnetic field. In a modulation-doped n-type structure all acceptors are ionized. An ionized acceptor acts as a repulsive center for a conduction electron. However, the latter cannot run away from the acceptor because it is confined in the z direction by the quantum well and in the x - y plane by the Lorentz force of magnetic field. The proposed states, whose energies occur above the free-electron Landau levels, were observed in interband photoluminescence by Vicente *et al.*¹¹

The present paper reports CR studies of conduction electrons in GaAs/Ga_{0.67}Al_{0.33}As heterostructures doped in the well with acceptors. We observe and discuss

effects related to single acceptors and disorder modes of the cyclotron resonance.

II. RESULTS AND DISCUSSION

Our four samples were modulation-doped asymmetric single quantum wells grown by molecular beam epitaxy. Sample 1 was a sample of reference similar to others but without a δ layer of Be acceptors. The other three samples are δ doped in the well with Be atoms. The samples characteristics are reported in Table I.

Samples were wedged to avoid interference effects. In most experiments the far infrared (FIR) optical transmission was measured at $T=1.8$ K in magnetic fields up to 13 T using a Fourier spectrometer. In order to minimize the background noise of the transmission spectra we took an average of 100 runs for each magnetic field.

Figure 1 shows FIR transmission spectra of the reference sample 1 for different magnetic fields. The standard cyclotron resonance is observed, its width slowly becomes narrower as the field increases. Figures 2–4 show the spectra for

TABLE I. Samples characteristics: d is the width of GaAs well, z_0 is the distance between δ layer and interface on the side of modulation doping; δ -Be is the density of Be acceptors in δ layer; N_s and μ are the electron density and mobility (at $T=1.8$ K), respectively.

Sample	d (nm)	z_0 (nm)	δ -Be $\times 10^{10}$ (cm ⁻²)	$N_s \times 10^{11}$ (cm ⁻²)	$\mu \times 10^4$ (cm ² V ⁻¹ s ⁻¹)
1	25			2.05	28.5
2	25	2	1	2.2	8.8
3	25	2	2	5.2	16
4	15	2	2	3.7	3.8

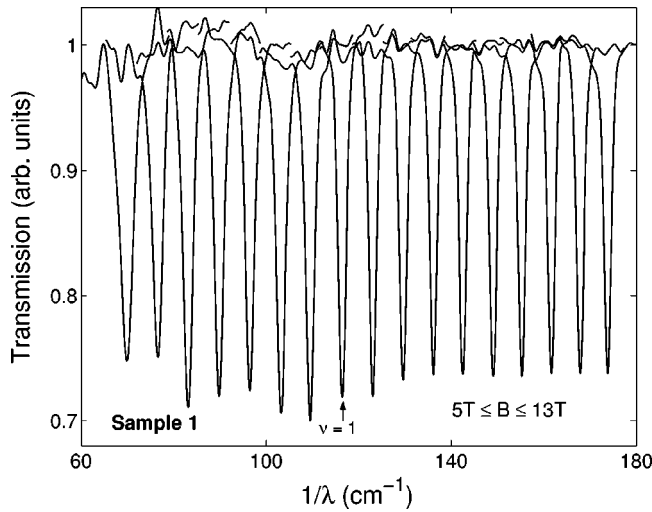


FIG. 1. Infrared transmission spectra at constant magnetic fields for the modulation-doped GaAs/Ga_{0.67}Al_{0.33}As sample 1, not intentionally doped with acceptors. The magnetic field increment is $\Delta B = 0.5$ T.

samples 2–4, respectively, which were δ doped with acceptors. It can be seen that their spectra are much richer than that of the reference sample. However, for the filling factors $\nu \leq 1$, the behavior of the undoped sample 1 and the weakly doped sample 2 become similar, as reported previously.^{5,7} For the Be doped samples, in addition to the CR transition, we observe a number of additional peaks. We find that the three samples doped with acceptors have similar spectra for comparable values of the filling factor. For example, it can be seen that the spectra for sample 2 at $\nu = 1.65$, for sample 3 at $\nu = 1.79$, and for sample 4 at $\nu = 1.61$ have quite similar forms.

In order to determine the transition energies we carried out a deconvolution of each spectrum using Gaussian peaks of variable amplitude and width. It can be seen from Figs. 5(a), 5(b) and 6 that the amplitudes of contributing peaks are

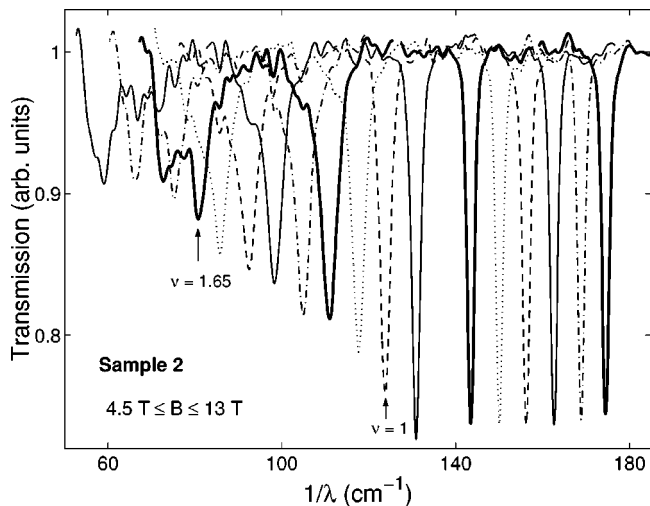


FIG. 2. Same as in Fig. 1, but for sample 2, intentionally doped with Be acceptors. Various spectra are marked with different lines for clarity.

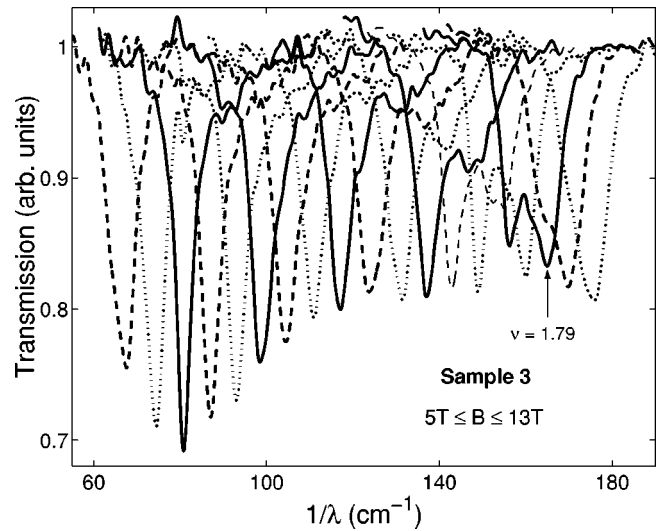


FIG. 3. Same as in Fig. 1, but for sample 3, intentionally doped with Be acceptors. Various spectra are marked with different lines for clarity.

considerably higher than those of the background peaks attributable to noise. We carefully checked that the contributing peaks had their correspondence at higher and lower fields. In addition, it was verified in a set of separate experiments at $1.8 \text{ K} < T < 8.5 \text{ K}$ that the main peaks did not change their positions with the temperature.

The energies of the observed transitions for sample 3 (counted from the CR energy) are shown in the upper part of Fig. 7 as functions of magnetic field B . The lower part of the figure shows the magnetotransport data obtained on the same sample under FIR illumination.

In order to describe the magnetoacceptor (MA) energies we follow Ref. 10. First, the screened repulsive Coulomb potential for the bulk is reduced to a 2D potential in the well by a variational ansatz. The screening of the potential does not include the effect of magnetic field, the polarization func-

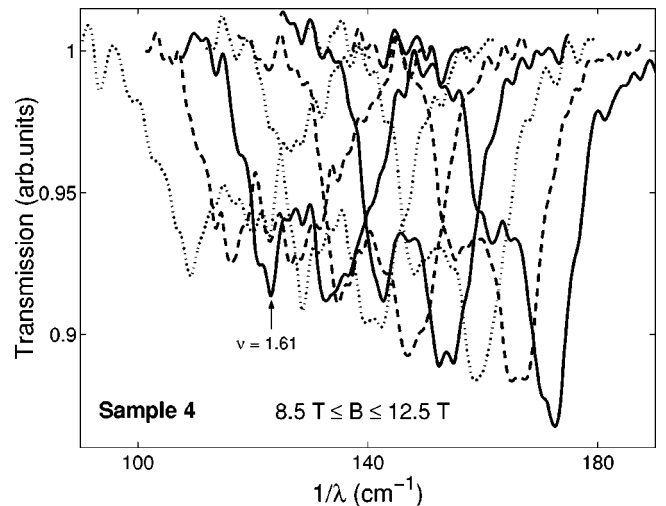


FIG. 4. Same as in Fig. 1, but for sample 4, intentionally doped with Be acceptors. Various spectra are marked with different lines for clarity. Two twinlike disorder modes are clearly observed.

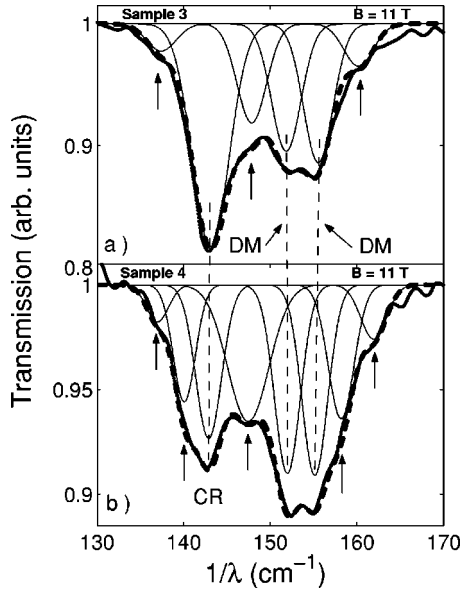


FIG. 5. Infrared transmission spectra for GaAs/Ga_{0.67}Al_{0.33}As quantum wells δ doped with $2 \times 10^{10} \text{ cm}^{-2}$ of Be acceptors at a magnetic field $B = 11 \text{ T}$. In addition to the cyclotron resonance (CR) and two disorder modes (DM) one observes a number of excitations evidenced by the deconvolution procedure. Solid lines—experiment, dashed lines—the sum of Gaussian peaks. Fig. 5(a)—sample 3, Fig. 5(b)—sample 4.

tion is taken in the form given by Ando, Fowler, and Stern¹² for the degenerate 2D gas. The static dielectric constant for GaAs is $\kappa_0 = 12.91$. Next, the energies of conduction electrons are calculated variationally using the trial functions

$$\Psi_{NM} = C_{NM} e^{iM\Phi} \eta^{|M|/2} e^{-\eta/2} L_N^M(\eta), \quad (1)$$

where $N = 0, 1, 2, \dots$, $M = \dots -1, 0, 1, \dots$ are quantum numbers, C_{NM} is the normalization factor, $\eta = \gamma \rho^2 a^2 / 2$, L_N^M are the associated Laguerre polynomials, a is the variational parameter, $\rho^2 = x^2 + y^2$, and $\gamma = \hbar \omega_c / 2R^*$.¹³ The resulting energies are higher than the Landau level (LL) energy ε_n to which the corresponding MA states “belong.” The effective 2D potential depends on the acceptor position in the well and

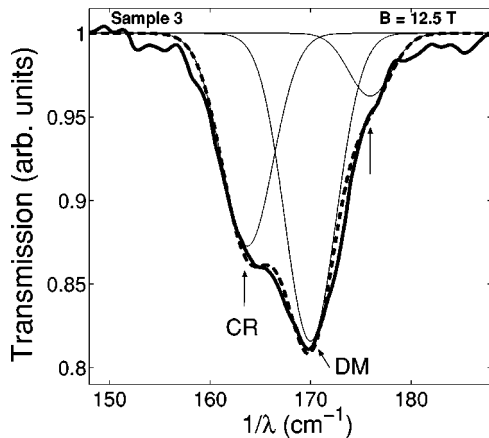


FIG. 6. Transmission spectrum and deconvolution peaks for sample 3 at $B = 12.5 \text{ T}$.

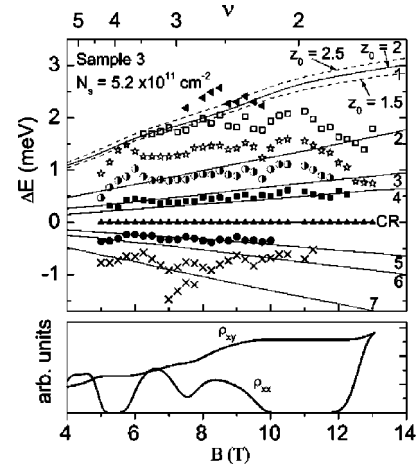


FIG. 7. Upper part: energies of magneto-optical transitions (counted from the CR energy) between magneto-acceptor (MA) and free electron Landau level (LL) states versus magnetic field intensity. Solid lines show the calculated energies for MA at $z_0 = 2 \text{ nm}$ from the interface. Tr1: LL($N=0, M=-1$) \rightarrow MA($N=1, M=0$); Tr2: LL($N=0, M=-2$) \rightarrow MA($N=1, M=-1$); Tr3: LL($N=0, M=-3$) \rightarrow MA($N=1, M=-2$); Tr4: LL($N=0, M=-4$) \rightarrow MA($N=1, M=-3$); Tr5: MA($N=0, M=-3$) \rightarrow LL($N=1, M=-2$); Tr6: MA($N=0, M=-2$) \rightarrow LL($N=1, M=-1$); Tr7: MA($N=0, M=-1$) \rightarrow LL($N=1, M=0$). Different symbols indicate experimental energies. Lower part: dc magnetotransport tensor components ρ_{xx} and ρ_{xy} vs B , measured on the same sample under FIR illumination.

the calculated MA energies exhibit a similar position dependence.¹⁰ For this reason, the theoretical transition energy 1, shown in Fig. 7, is indicated for three acceptor positions. The position dependence for other transitions is weaker. According to the selection rules, obtained with the functions (1), the transition energies can be both larger and smaller than the CR energy. The smaller energies correspond to transitions from MA states above LL n to the free electron state LL $n' = n + 1$, while the larger ones correspond to transitions from LL n to MA states above LL $n' = n + 1$. The selection rules are $\Delta M = \pm 1$ but the transitions $\Delta M = +1$ are much stronger. For free electron states the Landau number is $n = N + (M + |M|)/2$, so that all states with $M \leq 0$ have the same energy. Thus the selection rules allow, for example, transitions from LL state ($N=0, M=-1$) to MA state ($N=1, M=0$) or from MA ($N=0, M=-1$) to LL ($N=1, M=0$).

As indicated in the upper abscissa of Fig. 7, with increasing B the filling factor changes from $\nu \geq 4$ to $\nu < 2$. As a result, the optical transitions do not occur between the same states as B varies, but they shift from $(n=2) \rightarrow (n=3)$ at low values of B to $(n=0) \rightarrow (n=1)$ at high B . Since the MA binding energies depend on the Landau number n ,¹⁰ we calculate weighted averages of all transition energies as functions of B . This leads to a nonmonotonic slope of the energy 1 and tends to linearize other energies. The theory is compared with the experiment in the upper part of Fig. 7. It can be seen that two transitions: full squares above CR and full circles below CR can be attributed to the discrete states of conduction electrons bound to the ionized acceptors.

We identify the transition marked by stars as the disorder-shifted CR excitation [we call it disorder mode (DM)]. Considerations of optical excitations for the harmonic oscillator in a magnetic field lead to an absorption frequency $\omega_+^2 = \omega_i^2 + \omega_c^2$, where $\omega_c = eB/m_0^*$ is the cyclotron frequency and ω_i is the characteristic harmonic frequency related to the average distance between the acceptors.^{2,14} A typical excitation of this type is seen in Fig. 5(a) as the strong peak at $\hbar\omega = 155.4 \text{ cm}^{-1}$. For sample 3 this peak becomes comparable to CR at $B = 12 \text{ T}$, which corresponds to the filling factor $\nu < 2$. However, we find from the deconvolution procedure that this excitation begins to be observable at $B = 5 \text{ T}$, i.e., for $\nu \geq 4$.

This is an important finding, since until now the DM excitations were observed only at $\nu \leq 2$, see Refs. 1–9. This feature was never understood because it did not follow from the harmonic oscillator model.² At high fields, the DM peak tends to replace the CR peak, which is what one usually observes. We believe that also the transition marked with empty squares is a disorder mode. First, it is almost exactly parallel to the DM discussed above. Second, we observe on another sample two parallel DM peaks, see Figs. 5(b) and 10. Also the lower transition energy (half-filled circles in Fig. 7) is parallel to the main DM energy. At lower fields this energy corresponds well to the calculated transition energy 2, but at high fields it is lowered by the main DM excitation. The lowest transition energy (crosses) is almost parallel to the CR energy and its origin is not clear. Still, it occurs well within the range of calculated transition energies involving MA states.

It can be seen in Fig. 7 that the transition energies above CR have two maxima: first around $B \approx 5.7 \text{ T}$ and second at around 10.8 T . They correspond approximately to the filling factors $\nu = 4$ and $\nu = 2$, respectively, and result, in our understanding, from the oscillatory screening of the acceptor potentials by the 2DEG. Each time the Fermi energy is between the Landau levels the screening has a minimum and the interaction a maximum. This gives a maximum of energy for a transition having MA as the final state, which is what we observe. The oscillations of donor binding energy in similar structures were convincingly demonstrated by Raymond *et al.*¹⁵ Interestingly, the energy maxima in Fig. 7 occur also for the disorder modes. This corresponds well to the model of parabolic well formed by neighboring acceptor potentials. If the potentials are not screened, the well becomes narrower and the resulting oscillator frequency becomes higher.

The transmission curves for samples 3 and 4 shown in Figs. 5(a) and 5(b) are similar. Both exhibit CR, MA, and DM peaks. In particular, the spectrum in Fig. 5(b) for sample 4 confirms our identification of the two peaks above 150 cm^{-1} as DM modes. In general, the disorder introduced by acceptors in sample 4 is higher than that of sample 3, which is confirmed by the experimental mobility values at $T = 1.8 \text{ K}$ ($\mu = 3.8 \times 10^4 \text{ cm}^2/\text{Vs}$ and $16 \times 10^4 \text{ cm}^2/\text{Vs}$, respectively).

In principle, not only the transitions between free electrons and MA states (or vice versa) are possible but also the transitions between MA states associated to different LLs.

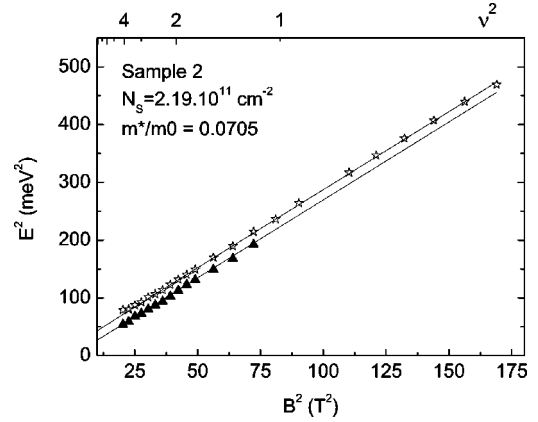


FIG. 8. Cyclotron resonance and disorder mode energies for sample 2 (energy square vs B^2). The solid lines are theoretical.

We checked this possibility but did not find experimental excitations having the corresponding energies. This should not be surprising since the number of MA states is lower than that of the free electron states, so that excitations between the MA states alone should be considerably weaker than those observed.

Now we turn to the disorder modes observed in our samples. Sample 2, which is rather weakly doped with acceptors, exhibits one disorder mode. As illustrated in Fig. 8, this mode follows quite well the standard parallel behavior to the CR energy in the $E^2(B^2)$ plot. On the other hand, as already discussed above, the more heavily doped sample 3 exhibits at least two (possibly even three) disorder modes. The energies of two DMs for this sample are shown in Fig. 9 together with the CR energy using the $E^2(B^2)$ plot. It can be seen that the characteristic parallel behavior of the energies is not perfect. Finally, in Fig. 10 we give similar plot for the heavily doped sample 4. Again, the parallel behavior is not perfect. Sample 4 exhibits a richer spectrum than sample 3, see Figs. 5(a) and 5(b), but the weaker excitations are not indicated in Fig. 10 for clarity.

The origin of multiple DM excitations is not clear. The standard picture of the oscillator frequency ω_i results from the acceptor potential fluctuations and the strong electron-electron interaction.^{16,17} There is no obvious reason why this

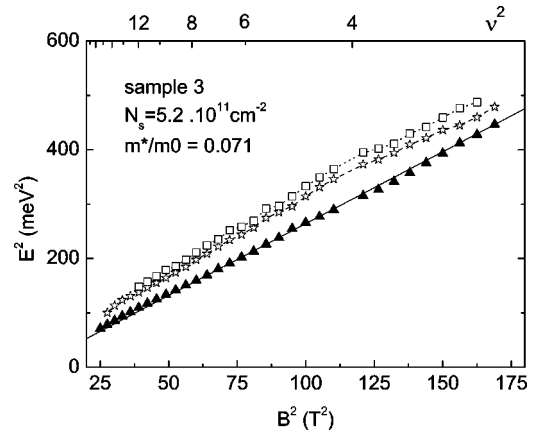


FIG. 9. Cyclotron resonance and disorder modes energies for sample 3 (energy square vs B^2). The straight line for CR is theoretical, the lines for DM's are drawn to guide the eye.

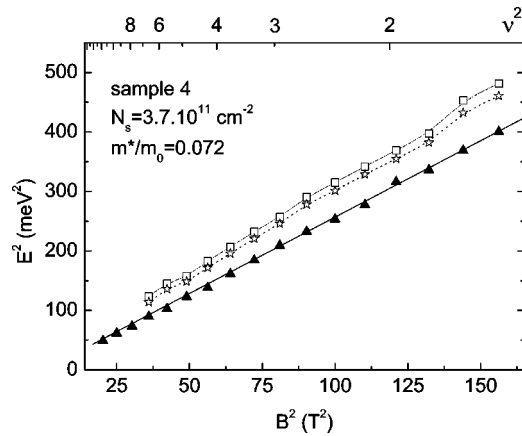


FIG. 10. Cyclotron resonance and disorder modes energies for sample 4 (energy square versus B^2). The straight line for CR is theoretical, the lines for DMs are drawn to guide the eye.

approach should give more than one oscillator frequency. Alternatively, two ω_i frequencies could come from two doping planes, one is introduced by the actual δ doping at 2 nm from the interface, the other results from the diffusion of Be atoms, probably at the GaAs/GaAlAs interface. In this case, however, the two frequencies should differ more from each other than what we observe, since the acceptor density at the second plane should be considerably lower than that of the

first. In a recent paper, Buth *et al.*¹⁸ reported an additional excitation between CR and DM, but its intensity was much lower than that of the DM peak.

We also investigated another heavily doped sample 5 ($N_s = 4.4 \times 10^{11} \text{ cm}^{-2}$ and $\delta\text{Be} = 4 \times 10^{10} \text{ cm}^{-2}$). It showed spectra similar to those showed above, in particular, two disorder modes were observed. The problem of multiple DM excitations requires further investigations.

III. SUMMARY

In summary, we observed and described states of conduction electrons in heterostructures bound to single ionized acceptors by a joint effect of the potential well and a magnetic field. Our results confirm the data of interband experiments. The magneto-optical energies show evidence of the oscillatory screening of acceptor potentials by 2D electron gas in a magnetic field. We also observed three effects related to the disorder modes of cyclotron resonance. First, two DMs are observed on three samples. Second, the DM energies show evidence for the resonant screening of the acceptor potentials. Third, at least one disorder mode begins to be observed at the filling factor $\nu \geq 4$, which contributes an important element missing until present in the harmonic oscillator model of DM excitations.

ACKNOWLEDGMENTS

We thank Dr. M. Sadowski for help in the experiments.

- ¹J.P. Kotthaus, G. Abstreiter, J.F. Koch, and R. Ranvaud, *Phys. Rev. Lett.* **34**, 151 (1975).
- ²B.A. Wilson, S.J. Allen, and D.C. Tsui, *Phys. Rev. B* **24**, 5887 (1981).
- ³J.P. Cheng and B.D. McCombe, *Phys. Rev. B* **44**, 3070 (1991).
- ⁴K. Ensslin, D. Heitmann, H. Sigg, and K. Ploog, *Phys. Rev. B* **36**, 8177 (1987).
- ⁵J. Richter, H. Sigg, K. v. Klitzing, and K. Ploog, *Phys. Rev. B* **39**, 6268 (1989).
- ⁶H. Sigg, J. Richter, K. v. Klitzing, and K. Ploog, in *High Magnetic Fields in Semiconductor Physics*, edited by G. Landwehr (Springer, Berlin, 1989), p. 419.
- ⁷R.J. Nicholas, M.A. Hopkins, D.J. Barnes, M.A. Brummell, H. Sigg, D. Heitmann, K. Ensslin, J.J. Harris, C.T. Foxon, and G. Weimann, *Phys. Rev. B* **39**, 10 955 (1989).
- ⁸G. Wiggins, R.J. Nicholas, J.J. Harris, C.T. Foxon, and G. Weimann, *Surf. Sci.* **229**, 488 (1990).
- ⁹M. Widmann, U. Merkt, M. Cortés, W. Häusler, and K. Eberl,

Physica B **249**, 762 (1998).

- ¹⁰M. Kubisa and W. Zawadzki, *Semicond. Sci. Technol.* **11**, 1263 (1996).
- ¹¹P. Vicente, A. Raymond, B. Couzinet, M. Kubisa, W. Zawadzki, B. Etienne, and M. Kamal Saadi, *Solid State Commun.* **96**, 901 (1995).
- ¹²T. Ando, A.B. Fowler, and F. Stern, *Rev. Mod. Phys.* **54**, 437 (1982).
- ¹³W. Zawadzki, X.N. Song, C.L. Littler, and D.G. Seiler, *Phys. Rev. B* **42**, 5260 (1990).
- ¹⁴H.J. Mikeska and H. Schmidt, *Z. Phys. B* **20**, 43 (1975).
- ¹⁵A. Raymond, B. Couzinet, M.I. Elmezouar, M. Kubisa, W. Zawadzki, and B. Etienne, *Europhys. Lett.* **43**, 337 (1998).
- ¹⁶E. Zaremba, *Phys. Rev. B* **44**, 1379 (1991).
- ¹⁷U. Merkt, *Phys. Rev. Lett.* **76**, 1134 (1996).
- ¹⁸K. Buth, M. Widmann, U. Merkt, E. Batke, and K. Eberl, *Physica E (Amsterdam)* **12**, 662 (2002).